ISSN 1330-3651 (Print), ISSN 1848-6339 (Online)
https://doi.org/10.17559/TV-20210906114213
Preliminary communication

Prediction of Vibration in the Discharge Ring of a River Type Hydroelectric Power Plant with Bulb Turbine Using Artificial Neural Networks and Support Vector Machine

Abdullah Emre ORAL*, Orhan Erdal AKAY

Abstract: Cracks are formed around the manhole covers located in the discharge ring areas of the turbine units of a hydroelectric power plant with a river-type bulb turbine due to the vibration of the units. Determining the operating parameters for the low vibration zone of the units to reduce or eliminate these cracks is an important issue in terms of reducing plant operating efficiency and maintenance costs. To solve this problem and to determine the central operating parameters in the safe vibration zone, a vibration prediction model was created with artificial neural networks and support vector machine. Operating parameters of the hydroelectric power plant; artificial neural networks and support vector machine were created to predict vibrations for each turbine unit using the water inlet-outlet height, network pollution level, power of each unit, total unit power, and vibration data from the discharge rings of the units. Vibration estimates were made based on operating parameters and compared with actual vibration values. The results obtained showed that the operating parameters for reducing the vibration values of the turbine units of the hydroelectric power plant could be determined practically with the help of artificial neural networks and support vector machine.

Keywords: artificial neural networks; hydroelectric power plants; support vector machine; turbine vibrations, vibration prediction

1 INTRODUCTION

There is a wide variety of studies carried out on hydroelectric power plants. A lot of work has been done to measure, monitor and predict models using artificial neural networks and mathematical models to solve various problems parameters.

River-type hydroelectric power plants are used in streams with wide plains and smooth routes and are generally not used for irrigation purposes due to their limited water capacity. In this type of power plant, the water inlet structures consist of vertical tunnels, and bulb-type turbines are used. These turbines have 4 or 5 blades and make the most of the river current. The axial flow-permitting design of the Bulb turbines allows keeping the turbine efficiency at the optimum level by tolerating low-angle flow deviations in the impeller blades at high specific speeds. On the other hand, vibration values are high in water discharge structures, especially since water does not come to turbine blades through the penstocks and similar structures [1, 2].

Mechanical vibrations, as is known, cause time-dependent fatigue in metal structures. This situation causes breakdown, wear, and efficiency losses in hydroelectric turbines. The vibrations of the discharge pipes and discharge rings of hydroelectric turbines take different values at different powers. The vibrations of the discharge pipe and discharge ring regions are generally dependent on the flow characteristics of the water and the pressure differences in the turbine wheels. Considering the studies, it is seen that most of the river-type hydroelectric power plants with bulb turbines have high vibration problems in their discharge systems. Especially in the discharge ring, where the water hits the impeller blades and rotates the turbine shaft, it is inevitable that there will be more vibration problems. Because in this region, the water loses its dynamic pressure by hitting the turbine blades, thus hydraulic energy creates a mechanical torque in the shaft. The formation of high different pressure zones at the water inlet-outlet of the impeller blades, the deterioration of the water flow, cause high vibrations in the discharge rings that protect the impeller blades [3-7].

Many studies have been carried out using various algorithms such as artificial neural networks (ANNs), deep learning, machine learning, gray wolf optimization in hydroelectric power plants. In these studies, estimation models of efficiency and power generation parameters of hydroelectric power plants were obtained and the factors affecting these parameters were analyzed. On the other hand, prediction models of vibrations occurring in hydroelectric turbine units have been obtained as well as the life expectancy of hydroelectric turbine shafts [8-18].

In addition to vibration measurement and evaluation of its results, mathematical models have been used to obtain numerical vibration results. The natural frequencies of hydroelectric turbine structures have been examined with mathematical models. Coupled dynamic mathematical models are developed, which consist of mutually coupled foundation vibrations, external random excitation of foundation, besides classical dynamics of nonlinear hydro-generator shaft system. Mathematical models have been developed for malfunctions that may occur due to vibration [19-22].

Figure 1 Crack samples on the discharge ring

The vibration-related problems observed in a Karkamış hydroelectric power plant with a river-type bulb turbine in Turkey, and the studies carried out to solve them are presented in this article. Vibrations are caused to the capillary cracks around the manhole covers at the discharge ring. Recurrent crack formations were detected in many body parts repaired by welding between 2015-2020. To repair these cracks, it is necessary to intervene by removing the relevant turbine unit, and this affects the operating efficiency and costs negatively. Two examples of the cracks described are presented in Fig.1, and the capillary crack region detected on the discharge ring is seen in the figure. Welding processes on the turbine units for crack removal were carried out according to the welding procedures given in the projects.

The main operating parameters of turbine units are water inlet-outlet levels, trash rack pollution, and the power of the turbine units is effective on vibration-induced crack formation. The study has been aimed to obtain a vibration prediction model, which is trained on the data of the main operating parameters of the hydroelectric power plant, in order to enable the turbines to be operated in low vibration regions.

2 MATERIAL and METHOD

2.1 Hydroelectric Power Plant

The study was carried out in Karkamış hydroelectric power plant with river-type bulb turbine units in Turkey (Fig. 2). This power plant has 6 identical bulb turbines, each with a capacity of 31.5 megawatts. The total installed power of the power plant is 189 megawatts and its annual electricity generation is 652 GWh/year. The dam reservoir is about 30 km long, 340 m high, the lake area is 28.4 km² and the lake volume is 156.9 million m³ [23-24].

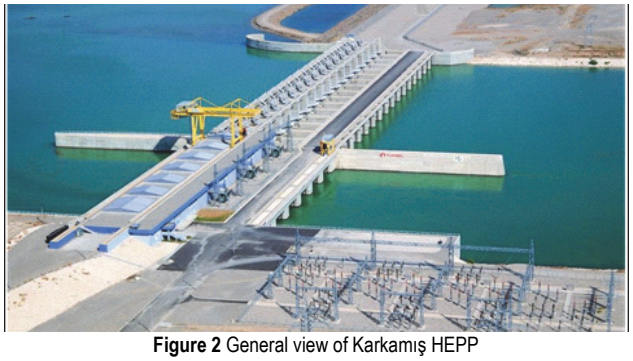

Figure 2 General view of Karkamış HEPP

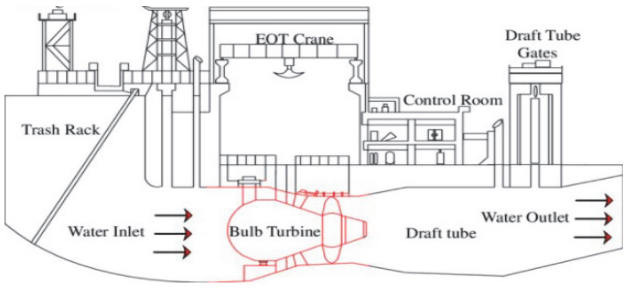

Figure 3 Hydroelectric power plant cross-section

Bulb-type turbines operating in the hydroelectric power plant are positioned at horizontal height, and turbine centers are placed side by side with an average of 30 meters intervals. The water inlets of the turbines of the units are independent of each other. The typical cross-section of hydroelectric power plant with river-type bulb turbine units is presented in Fig. 3 [5].

There are water inlet grids for each turbine unit in the hydroelectric power plant (Fig. 4). The distance between the two grids is 4 m. The sensors that measure the level of grid contamination are of the same type and characteristics as the water inlet and outlet sensors. Each unit has 2 hydrostatic level sensors located on the grid water inlet and water outlet side. There is a total of 10 sensors on the grid water inlet and grid water outlet sides of the 5 turbine units where the data is taken. The sensors of each unit are independent. In the SCADA system, the pollution level is read in meters. SCADA system carries out processes such as data collection, recording, viewing, and decision-making. Activation, deactivation, and working power of turbine units are controlled by the SCADA system.

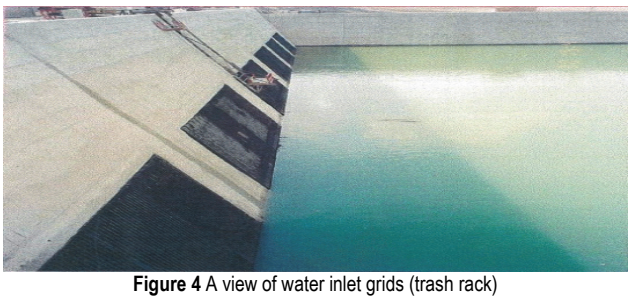

Figure 4 A view of water inlet grids (trash rack)

Turbine units do not have sensors to measure vibrations perpendicular to the flow direction of the water in the discharging ring. For this reason, vibration sensors are installed in the discharge ring of each turbine unit. The vibration sensor mount principle and a sample photograph of the mounted sensor to the turbine unit are presented in Fig. 5. Vibration sensors on the discharge rings of each unit transfer 4-20 mA direct current signals to the vibration measurement monitoring system.

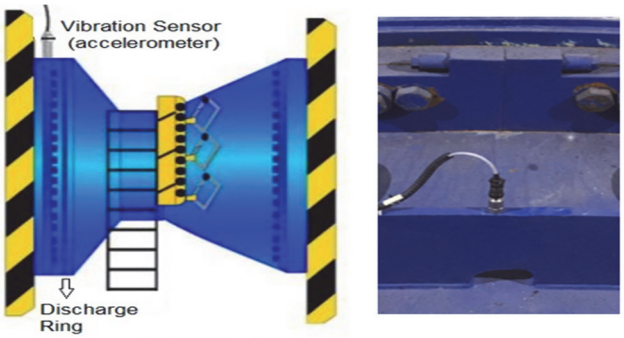

Figure 5 Vibration sensor installations

The basic technical specifications of the water inlet-outlet level, trash rack pollution, and vibration sensors whose data are used in the study are listed in Tab. 1 [25-26].

Table 1 Main specifications of some sensors

Type	Water Inlet-Outlet Level and Trash Rack Pollution Sensors	Vibration Sensors
Principle	Hydrostatic piezorezistif immersion prob	Accerolometer
Range	0-10-meter water column	2-10000 Hz
Accuracy	0.1% FS	±10% 100 mV/g
Current	4-20 mA	2-20 mA

2.1 Data Collection and Analysis

The data of 5 turbine units were used in the study. Measurable variables that have an effect on pressure changes in turbine units have been selected. Independent variables used as input are water inlet-outlet levels, turbine unit power, total power, and trash rack pollution. The absolute vibration in the discharge rings of the discharge tube of each unit and in the direction perpendicular to the water flow direction was taken as the dependent variable to be estimated by the ANNs and support vector machines (SVM).

2.1.1 Artificial Neural Networks

Since the water inlets of the units are independent (Fig. 4), separate ANNs were created for each unit. The data average of the 5 units from which the data was taken was not used. The neural network model designed for five independent inputs and one dependent output parameter is given below in Fig. 6.

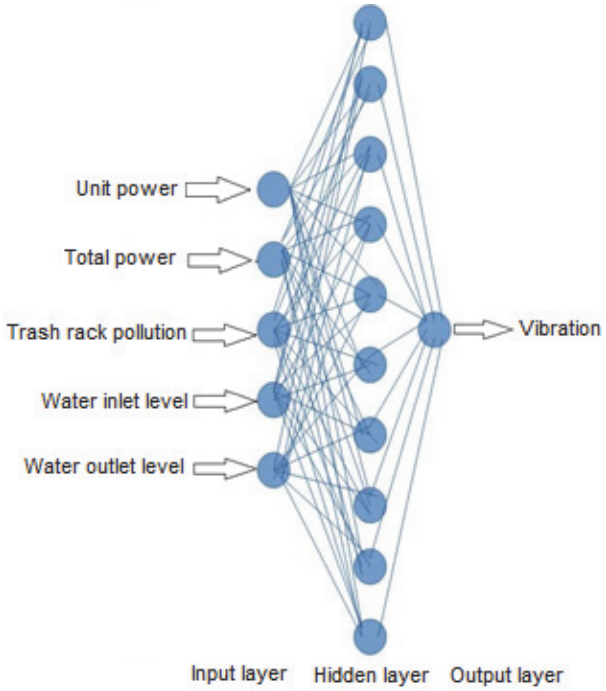

Figure 6 Neural network model

One of the popular training algorithms used in ANN applications is the feedforward backpropagation algorithm. This algorithm is effective in training complex and nonlinear ANNs. Its main purpose is to minimize the error between the output generated from the network and the input values [33-34]. The number of hidden neurons was determined to be 2 times the input parameters [35]. The hyperbolic tangent sigmoid function, which is one of the two most used functions in applications, is used as a transfer function in the hidden layer and output layer [36]. The mean square error (MSE) method is the most frequently used estimation accuracy criteria. The ability to decompose the estimation error into variance sums is an important advantage of this criterion [33].

Constituting the ANN architecture; numbers of layers and neurons, transfer functions, etc. There are no specific rules for choosing and they are determined by experience and/or trial-and-error methods [37-41]. Combinations of different parameters were tried in the creation of the ANNs used in this study, and the parameters with the best *MSE* and *R* performance results were used. These parameters used in ANNs are given in Tab. 2.

Table 2 Neural network structure and parameters

Input layer	1
Hidden layer	1
Output layer	1
Input neuron	5
Hidden layer neuron	10
Output neuron	1
Weight	Random
Summation junction	$\sum_{i=1}^{n} Xi \cdot Wi$
Hidden layer transfer function	Hyperbolic tangent sigmoid
Output layer transfer Function	Hyperbolic tangent sigmoid
Network Type	Feed forward backpropagation
Performance analysis 1	Mean square error (*MSE*)
Performance analysis 2	Correlation coefficient (*R*)

Mean squares of error (*MSE*) and (*R*) Pearson correlation coefficients were used in the study for model performance analysis. The measured value is Y_t and the output from the model is F_t in Eq. (1). Also $\bar{x}$ is the mean of the *x* series, and $\bar{y}$ is the mean of the *y* series in Eq. (2). [28]

$$MSE = \frac{1}{n}\sum_{t=1}^{n}(Y_t - F_t)^2 \tag{1}$$

$$R = \frac{\sum (x-\bar{x})\,(y-\bar{y})}{\sqrt{\sum (x-\bar{x})^2 \sum (y-\bar{y})^2}} \tag{2}$$

In April and August 2020, data were collected from turbine units 1-5 in 11 days. Since the month with the lowest flow rate of the river in August and the highest month is April, data were taken in these months in order to examine the effect of the maximum and minimum conditions in the study. For each turbine unit 5 dependent and 1 independent variable, 264 data were taken and a total of 1584 (6 × 264) data were used for training a network, and a total of 7920 data (5 × 1584) for 5 turbine units. The independent variable data of the units were taken from the SCADA system [26] and the dependent variable vibration data were taken from the central vibration monitoring systems [27]. Of the collected 1584 pieces of data 70% were used as training, 15% as validation, and 15% as test data.

The Matlab-nntool module for training was used as the training algorithm with the Levenberg-Marquardt algorithm. The Levenberg-Marquardt algorithm was preferred because of the speed and stability it provides in the training of ANNs. The sample Matlab interface of the Turbine unit-1 network model trained using the Matlab-nntool module is presented in Fig. 7. Information on the algorithm and performance criteria used in the formation of the network are seen in this Matlab interface.

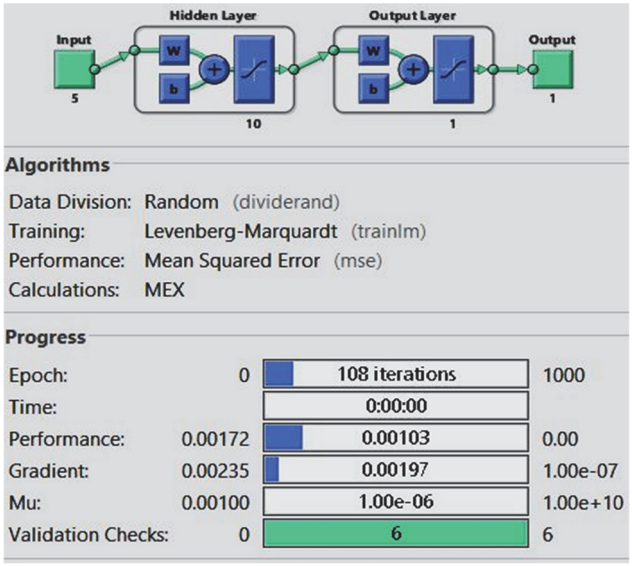

Figure 7 Turbine Unit-1 sample network model

2.1.2 Support Vector Machine Algorithm

SVM is a machine learning approach in data-driven research areas established by Cortes and Vapnik [29]. SVM is based on statistical learning theory. SVM is mainly used to best distinguish between two classes of data. For this purpose, decision boundaries or hyperplanes are determined. In a nonlinear dataset, SVMs cannot plot a linear hyperplane. That is why Kernel functions are used. The kernel method greatly enhances machine learning on non-linear data [30]. The operation of the SVM estimator (y) is expressed as follows [30]:

$$y = (K_{xi}\ W_{jk}) + b \tag{3}$$

If the Kernel function is K_{xi}, b is the bias term of the SVM network and is called the weight vector W_{jk}. K_x and W represent Lagrange multipliers. K_{xi} is a nonlinear function that maps input vectors to a high-dimensional feature space. Kernel (K_{xi}) is determined by various function solutions. In this study, radial basis function (RBF), polynomial, and PUK kernel functions are used. The SVM kernel functions and their parameters used to estimate the vibration values of the units are shown in Tab. 3 [31-32].

Table 3 The PUK kernel function and parameters used in DVM

Kernel Function	Formulas	Parameters
Pearson VII (PUK) Kernel	$K(x,y) = \frac{1}{\left[1 + \left(\frac{2\sqrt{\lVert x-y\rVert^2}\sqrt{2^{(1/\omega)}-1}}{\sigma}\right)^2\right]^{\omega}}$	(ω, σ) Pearson width parameters
Polynomial Kernel	$K(x,y) = \left((x \cdot y) + 1\right)^d$	(d) Polynomial grade
The Radial-Based Function (RBF) Kernel	$K(x,y) = e^{-\gamma(x-xi)^2}$	(γ) Kernel dimension

3 RESULTS

Using the data collected in the study, ANNs were created for five-turbine units. The MSE plot of the turbine unit-1 for training, validation, and testing is presented in Fig. 8.

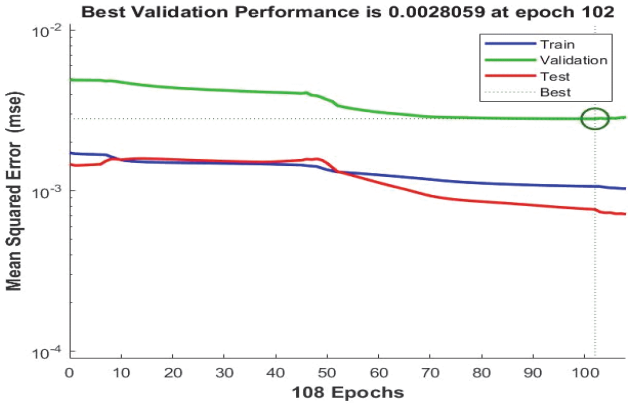

Figure 8 Turbine unit-1 the mean square error (*MSE*)

Correlation coefficient values (R) of the training, validation, and test sets were obtained for turbine unit-1 (Fig. 9). The obtained R values are very close to the ideal value. In these graphs, the horizontal axis shows the vibration data used to train the artificial neural network, and the vertical axis shows the predicted vibration values by the ANNs.

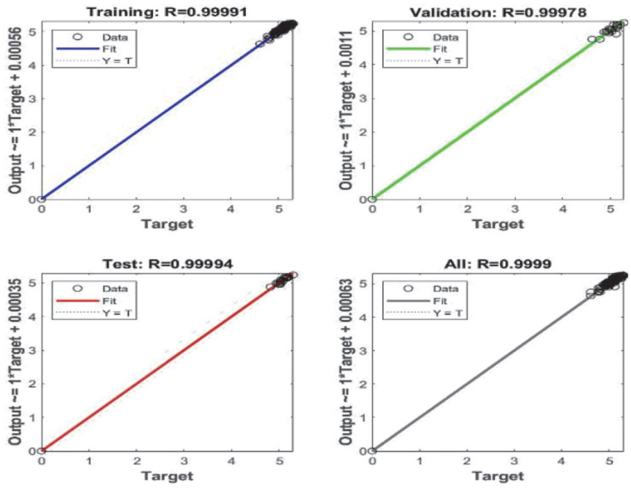

Figure 9 Turbine unit-1 correlation coefficient values (R)

MSE and R values for the turbine units-(1-5) are obtained and presented in Tab. 4.

Table 4 According to ANNs turbine units *MSE* and R values

Turbine unit	*MSE*	R
1	0.0028	0.9999
2	0.00285	0.9995
3	1673.993	0.6735
4	0.00472	0.9995
5	0.0167	0.9189

MSE and R values in this table are quite satisfactory, except for turbine unit-3. The low-performance values for turbine unit-3 are related to the accuracy of the data used in training the network. It has been observed that some trash rack pollution data of April and August 2020 used in the ANN of turbine unit-3 have negative values. It is not

possible for the trash rack pollution value to be a negative value. This situation has been caused by the calibration fault of the pressure sensors measuring the trash-rack pollution level or the pollution sensor.

ANNs created for turbine units 1-2, 3, and 5 have been asked to make vibration predictions using data that the networks did not recognize before. For this purpose, 360 independent input data are collected in 24-hour periods for each of the turbine units 1-2, 3, and 5 on September 2-4, 2020 (turbine unit 4 was not operated). ANN models are run by entering the independent variable data for these turbine units and 72 vibration predictions are made for turbine units 1-2, 3, and 5 at one-hour intervals. The graphs comparing the estimated vibration values of the nets of the turbine units with the actual vibration values measured on the discharge rings are presented in Figs. 10 to 13.

The vibration values estimated by ANN and the actual vibration values of turbine unit-1 are very close to each other; this situation is seen in Fig. 10. As a result, the performance quality of the ANN created for turbine unit-1 and the vibration values estimated by the networks in real operating conditions are obtained quite compatible.

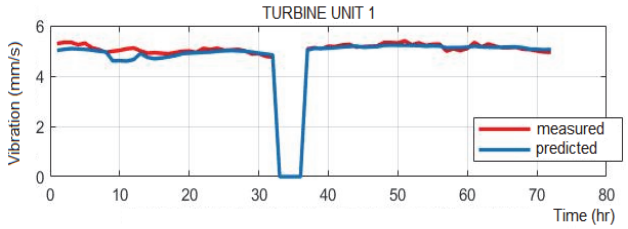

Figure 10 Turbine unit-1 predicted-measured vibration comparison

Although the *MSE* and *R* performances for turbine unit-2 are quite satisfactory, the accuracy of the vibration values estimated by the ANN is low in the range of data sets 34-38. It is predicted that this situation is related to the data taken in April and August to create the ANN. In April and August, the turbine unit-2 was operated in the power range of 20-22 megawatts, and data in the range of 20-22 MW were often used in the training and creation of ANNs. However, since the vibration values that the ANN of the turbine unit-2 wanted to predict in the 34-38-hour range were for 18 MW of power, the prediction performance obtained was quite low (Fig. 11).

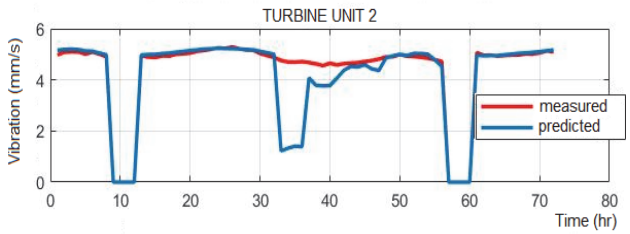

Figure 11 Turbine unit-2 predicted-measured vibration comparison

The vibration values estimated by ANN and the actual vibration values of turbine unit-3, whose *MSE* and *R* are quite low, are far from each other. It is predicted that this situation is caused by the faulty trash-rack pollution data used for training the ANN (Fig. 12).

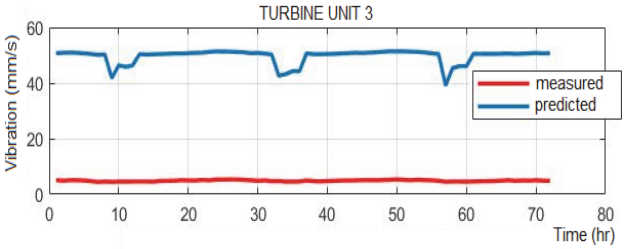

Figure 12 Turbine unit-3 predicted-measured vibration comparison

The graphs of predicted vibration values, and actual vibration values of turbine unit-5, which have slightly lowered *MSE* and *R* according to turbine unit-1, are slightly more inconsistent than the graph in turbine unit-1. This shows that the performance quality of the ANNs belonging to turbine unit-5 *MSE* and *R* values are lower than those of unit-1. For this reason, the accuracy of the vibration values estimated under real operating conditions is consistent (Fig. 13).

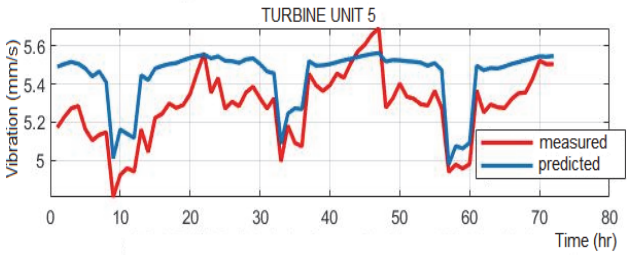

Figure 13 Turbine unit-5 predicted-measured vibration comparison

Vibration estimation was made with artificial neural networks for turbine units (1, 2, 3, 5) using independent variables corresponding to randomly taken vibration values in September 2020. The results of this study are given in Tab. 4. Total power is 81.3028 mW, water inlet level is 338.641 m, water outlet level 329.4075 mm, are the working parameters not given in this table. As can be seen from this table, the deviation in the predicted and measured vibration values for turbine units 1 and 5 was obtained with quite acceptable errors of −0.014% and 1.02%, respectively. A deviation of 18.79% was obtained for turbine unit-2. The results obtained with turbine unit 3 are incomparable. These deviations confirm the explanations made for Figs. 10 to 13.

Table 4 Predicted and measured vibration comparison

Turbine Unit	Turbine Unit Power / mW	Trash Rack Pollution / m	Predicted Vibration / mm/s	Measured Vibration / mm/s
1	20.1527	0.5150	5.1094	5.1818
2	18.5848	0.9635	3.7771	4.6515
3	20.7268	0.8043	50.4290	4.7560
5	21.8384	0.1388	5.5038	5.3926

Seventy-two vibration data, which were requested to be estimated from artificial neural networks for September 2020, were also estimated using the support vector machine method. The performance values of the Kernel functions used in the support vector machine method are given in Tab. 5.

In Figs. 14 to 16, graphs showing the relationship between the vibration prediction values of the Kernel functions for unit-1 and the actual vibration values are given.

Table 5 Kernel functions performance

	Unit-1			Unit-2			Unit-3			Unit-5		
Error analysis	The polynomial kernel (PK)	The PUK kernel (PUKK)	The RBF kernel (RBFK)	PK	PUKK	RBFK	PK	PUKK	RBFK	PK	PUKK	RBFK
Correlation coefficient	0.999	0.9975	0.991	0.992	0.999	0.988	0.774	0.812	0.811	0.860	0.892	0.876
Mean Square Error	0.1087	0.0403	0.272	0.115	0.133	0.645	0.137	0.171	0.195	0.233	0.142	0.145

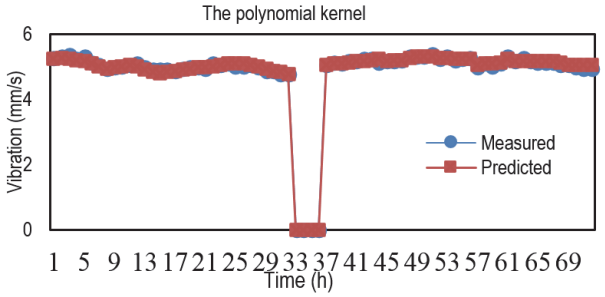

Figure 14 Prediction of unit-1 vibration SVM Polynomial Kernel

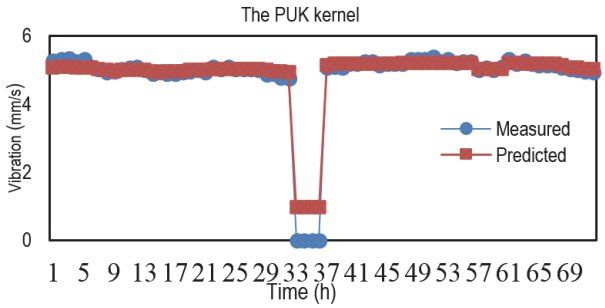

Figure 15 Prediction of unit-1 vibration SVM The PUK Kernel

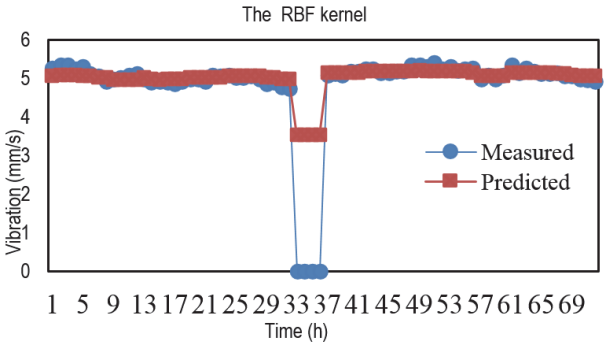

Figure 16 Prediction of unit-1 vibration SVM The RBF Kernel

Looking at the results obtained, it is seen that the estimated and measured vibration data presented in Figs. 14 to 16 are generally in good agreement. It can be seen that the estimation results presented in Figs. 15 and 16 of the data set in the 34-38 time interval are relatively poor compared to the estimation results presented in Fig. 14.

4 CONCLUSIONS

The vibration values estimated by the used ANNs have increased, depend on total unit power and single-unit power, the water inlet-output level difference, and the network pollution values. Due to measurement errors, an insufficient number of data, and different operating parameters, vibration estimation for all turbine units could not be made with the desired accuracy with ANN models. In addition to these, the effect of working combinations of turbine units on vibration outputs was not investigated. Feeding ANNs with more data on different conditions will increase the accuracy of the predictions. At the same time, regular calibration of the sensors is very important for the networks to make accurate predictions.

In addition to the ANNs, the vibrations of the units were also estimated using the support vector machine method. The performance values of the two methods show quite a parallelism, as seen in Tab. 4 and Tab. 5. Especially for unit-1, very close results were found in the two methods.

This study showed that vibration estimation can be made using ANNs and SVM in a river-type hydroelectric power plant with a bulb turbine. It has been seen that the operating parameters for reducing the vibration values of the turbine units of the river-type hydroelectric power plant will be determined and are practically applicable.

Thus, it is aimed to reduce the body cracks due to fatigue in the water discharge structures of turbine units, to increase the operating efficiency of the hydroelectric power plant by reducing the time and costs spent on the repair of these cracks.

Acknowledgements

This study was prepared under the supervision of the second author, using the Master's Thesis of the first author.

The authors of this study, for their support, would like to thank the Turkish Electricity Generation Corporation, Energy Efficiency Department, R&D Directorate, and Karkamış hydroelectric power plant Operation Directorate.

5 REFERENCES

[1] Özdemir, M., Dalcalı, A., & Ocak, C. (2020). Run of river Hydroelectric Power Plants and Turbine - Generators used in These Power Plants. *BJESR Journal Engineering Sciences and Researchers*, *2*(2), 69-75.

[2] Oral, F., Behçet, R., & Aykut, K. (2017). The Assessment of Hydroelectric Power Plant Reservoir Data with the Purpose of Energy Production. *BEU Journal of Science*, *6*(2), 29-38.

[3] Sridharan, P. (2016). Vibration Analysis and Mitigation Techniques For Bulb Turbine in Small Hydroelectic Power Plants. *International Journal of Advanced Engineering and Technology*, *VII*(I), 80-84.

[4] Türkmenoğlu, V. (2013). The vortex effect of Francis turbine in electric power generation. *Turkish Journal of Electrical Engineering and Computer Sciences*, *21*, 26-37. https://doi:10.3906/elk-1105-45

[5] Sridharan, P. & Kuppuswamy, N. (2014). Mitigation of Vibration on Bulb Turbine in Small Hydro Electric Power Plants. *International Journal of Engineering and Technology (IJET)*, *5*.

[6] Yaseen, Z., Ameen, A., Aldlemy, M., Ali, M., Afan, H., Zhu, S., Al- Janabi, A., Ansari, N., Tiyasha, T., & Tao, H. (2020). State-of-the Art-Powerhouse, Dam Structure, and Turbine Operation and Vibrations. *Sustainability*, *12*, 1676.

https://doi:10.3390/su12041676
[7] Mohanta, R., Chelliah, T., Allamsetty, S., Akula, A. & Ghosh, R. (2017). Sources of vibration and their treatment in hydro power stations-A review. *Engineering Science and Technology, an International Journal*, *20*(2017), 637-648. https://doi.org/10.1016/j.jestch.2016.11.004
[8] İnallı, K., Işık, E., & Dağtekin, İ. (2014). The prediction of efficiency and production parameters in Karakaya hpp using the artificial network. *Dicle University Journal of Engineering*, *5*(1), 59-68.
[9] Karakuş, M. & Altın, C. (2014). Yield of the Hydroelectric Power Plant using Feed Forward and Recurrent Neural Networks: Hirfanlı Dam Application Example. *Electronic Letters on Science & Engineering*, *10*(2), 1305-8614.
[10] Hammid, A., Sulaiman, M., & Abdalla, A. (2018). Predictionofsmall hydropower plant power production in Himreen Lake dam (HLD) using artifical neural network. *Alexandria Engineering Journal*, *57*, 211-221. https://doi.org/10.1016/j.aej.2016.12.011
[11] Makas, Y. & Karaatlı, M. (2016). Suleyman Demirel University. *The Journal of Faculty of Economics and Administrative Sciences*, *21*(3), 757-772.
[12] Zhao, W., Egusquiza., Valero, C., Valentin, D., Presas, A., & Egusquiza, E. (2020). On the use of artificial neural networks for condition monitoring of pump-turbines with extended operation. *Measurement*, *163*, 107952. https://doi.org/10.1016/j.measurement.2020.107952
[13] Liao, G.-P., Gao, W., Yang, G., & Guo, M.-F. (2019). Hydroelectric Generating Unit Fault Diagnosis Using 1-D Convolutional Neural Network and Gated Reccurent Unit in Small Hydro. *IEEE Sensors Journal*, *19*(20).
[14] Ilıć, D., Mıloševıć, D., Jovanovıć, Z., & Vulić, M. (2021). MLP ANN Condition Assessment Model of the Turbogenerator Shaft A6 HPP Đerdap 2. *Tehnički vjesnik*, *28*(1), 291-296. https://doi.org/10.17559/TV-20190510052210
[15] Hu, X., Li, C., & Tang, G. (2019). A Hybrid Model For Predicting The Degradation Trend Of Hydropower Units Based On Deep Learning. *2019 Prognostics & System Health Management Conference.*
[16] Condemi, C., Pérez, D., Mastoreni, L., Fernández, S., & Salcedo-Sanz, S. (2021). Hydro-power production capacity prediction based on machine learning regression techniques. https://doi.org/10.1016/j.knosys.2021.107012
[17] Fu, W., Wang, K., Tan, J., & Shao, K. (2020). Vibration Tendency Prediction Approach for Hydropower Generator Fused with Multiscale Dominant Ingredient Chaotic Analysis, Adaptive Mutation Grey Wolf Optimizer, and KELM. *Hindawi Complexity*, *2020*, 20. https://doi.org/10.1155/2020/4516132
[18] Sun, W. & Guo, Z. (2021). Mathematical modeling and nonlinear vibration analysis of a coupled hydro-generator shaft-foundation system. https://doi.org/10.1016/j.cnsns.2021.105776
[19] Hatiegan, C., Pădureanu., Jurcu., M., Nedeloni, M., Hamat, C., Chioncel, C., Trocaru, S., Vasile, O., Bădescu, O., Micliuc, D., Nedeloni, L., Băra, A., & Haţiegan, L. (2017). Vibration analysis of a hydro generator for different operatin regimes. *IOP Conf. Series: Materials Science and Engineering*, *163*, 012030. https:// doi:10.1088/1757-899X/163/1/012030
[20] Sperber, C., Weber, W., & Eberhard, P (2019). Numerical Anlysis of Vibration Patterns in Hydropower Units. https://doi.org/10.1002/pamm.201900036
[21] Kahraman, G. & Özdemir, O. (2021). Mathematical modeling of vibration failure caused by balancing effect in hydraulic. *Mechanics Basics Design of Structures an Machines*. https://doi.org/10.1080/15397734.2021.1873148
[22] See https://www.euas.gov.tr/tr-TR/santraller/karkamis-hes
[23] See https://voith.com/corp-en/BulbPitS-Turbines_Generators.pdf
[24] See https://ctconline.com/products/ctc-line/industrial-accelerometers/100-mv-g-standard-size/?prd=AC102
[25] See https://rittmeyer.com/en/instrumentation/products/level-sensors#c2610
[26] See https://ee.mam.tubitak.gov.tr/sites/images/ee_mam/karkamis_hepp_project_info_0.pdf
[27] See http://www.vibsens.com/index.php/products/condition-monitoring-systems/v6000-large-sized-machinery-protection-system
[28] Schober, P., Boer, C. S., & Lothar, A. (2018). Correlation Coefficients: Appropriate Use and Interpretation. *Anesthesia & Analgesia*, *126*(5), 1763-1768. https://doi.org/10.1007/BF00994018
[29] Cortes, C. & Vapnik, V. (1995). Support-vector networks. *Machine learning*, *20*(3), 273-297.
[30] Hsu, C. W., Chang, C. C., & Lin, C. J. (2003). A practical guide to support vector classification.
[31] Schölkopf, B., Burges, C. J. C., & Smola, A. J. (1999). *Advances in kernel methods: support vector learning*. MIT press. https://doi.org/10.1109/72.870050
[32] Shevade, S. K., Keerthi, S. S., Bhattacharyya, C., & Murthy, K. R. K. (1999). Improvements to the SMO Algorithm for SVM Regression. *IEEE Transactions on Neural Networks*, *11*(5), 1188-1193. https://doi.org/10.1016/S0169-2070(97)00044-7
[33] Zhang, G., Patuwo B. E., & Hu, M. Y., (1998). Forecasting with artifical neural networks, the state of the art. *International Journal of Forecasting*, *14*(1), 35-62.
[34] Verbos, P. J. (1994). *The roots of backpropaagation: From ordered derivatives to neural networks and political forecasting*. John Wiley & Sons. https://doi.org/10.1016/0925-2312(91)90045-D
[35] Wong, F. S. (1991). Time seies forecasting using bacpropagationneural networks. *Neurocomputing*, *2*(4), 147-159.
[36] Demuth, H. & Beale, M. (2000). Neural network toolbox user's guide. https://doi.org/10.1108/imds.2000.100.5.245.2
[37] Berry, M. A. & Linoff, G. S. (2000). Mastering data mining: The art of science of customer relationship management, *Industrial Management & Data Systems*, *100*(5), 245-246.
[38] Şen, Z. (2004). *Yapay sinir ağları ilkeleri*. Su Vakfı Yayınları.
[39] Öztemel, E. (2012). *Yapay sinir ağları*. Papatya Yayıncılık, İstanbul.
[40] Hu, C. (2002). *Advanced tourism demand forecasting: ANN and Box-Jenkins Modelling*. Doctoral dissertation, Purdue University, MI, USA.
[41] Tu, J. V. (1996). Advantages and disadvantages of using artifical neural networks versus logistic regression for predicting medical outcomes. *Journal of clinical epidemiology*, *49*(11), 1225-1231. https://doi.org/10.1016/S0895-4356(96)00002-9

Contact information:

Orhan Erdal AKAY, PhD, Assistant Professor
(Corresponding author)
Kahramanmaraş Sütçü İmam University,
Department of Mechanical Engineering,
46040 - Onikişubat, Kahramanmaraş, Turkey
E-mail: akayorhan@ksu.edu.tr

Abdullah Emre ORAL, MSc Student
Kahramanmaraş Sütçü İmam University,
Department of Mechanical Engineering,
46040 - Onikişubat, Kahramanmaraş, Turkey
E-mail: akayorhan@ksu.edu.tr